Submitted on
October 5, 1994
to the. Journal of Chemical Physics

Association Reactions at low Pressure,

5. The CH_3^+/HCN System. A Final Word?.

Vincent G. Anicich, Atish D. Sen,[a] and Wesley T. Huntress, Jr.

Jet Propulsion I laboratory,
California Institute of Technology,
4800" Oak Grove Drive.,
Pasadena, CA 91109.

Murray **J. McEwan,[b]**

Department of Chemistry,
University of Canterbury
Christchurch, New Zealand.

a NRC-NASA Research Associate, at JPL 1989.
b NRC-NASA Research Associate at JPL 1993,

ABSTRACT

The reaction of the methyl cation with hydrogen cyanide is revisited. We have confidence that we have re.solved a long standing apparent contradiction of experimental results. A literature history is presented along with one new experiment and a reexamination of an old experiment. In this present work it is shown that all of the previous studies had made consistent observations. Yet, each of the previous studies failed t o observe all of the information present. The methyl cation does react with HCN by radiative association, a fact which had been in doubt. The product ions formed in the two-body and three-body processes react differently with HCN. The collisionally stabilized association product formed by a three-body mechanism, does not react with HCN and is readily detected in the experiments. The radiatively stabilized association product, formed by a slow two-body reaction, is not detected because i t reacts with HCN by a fast proton transfer reaction forming the proton ated HCN ion. Previous studies either 'lost' this product in the extremely large proton ated HCN signal that is always present when HCN is used, o r discounted it for various reasons. We have been able to show by ion cyclotron resonance (ICR) techniques (both FT-ICR and tandem ICR-Dempster-ICR) that the radiative association product does react with t h e HCN to form the protonated HCN ion.

INTRODUCTION

The reaction between CH_3^+ and HCN was reported in 1979[1] to have a radiative association mechanism. In that original work two pieces o f information were used to make the deduction. It was observed that the number of CH_3^+ ions at 15 Daltons, decreased with time by a second order process with a rate that was proportional to the product of the two concentrations: $[CH_3^+]$ and [HCN]. A bimolecular reaction rate coefficient based on the removal of CH_3^+ of, $k_2 = 2$ x 10-10 $cm^3 s^{-1}$, was measured a t $\sim 10^{-7}$ Torr and at -- 100 ms. The other piece of information was that a t $\sim 10^{-5}$ Torr and after a drift time of ~ 1 ms, the product ion, $C_2H_4N^+$, was identified using double resonance techniques. It was therefore deduced that the reaction removing CH_3^+ could be written as

$$CH_3^+ + HCN \rightarrow CH_3NCH^+ + h\nu \qquad (1)$$

A year later after continued study it was determined that the same reactants also had a competing three- body stabilization mechanism[2]. It was determined that a second mechanism exhibited third order kinetics with a measured bimolecular reaction rate coefficient that was dependent on the pressure. It was therefore deduced that a second association reaction could be written as

$$CH_3^+ + HCN + M \rightarrow CH_3NCH^+ + M \qquad (2')$$

It was assumed in the second study that the double resonance identification of the association product under the three-body conditions Reactions (2) also applied to the bimolecular radiative. association reaction (Reaction (1)).

The reaction rate coefficient for Reaction (2) when He was he third-body, M, was reported as k3 = 5 x ()-25 $cm^6 s^{-1}$. This observation is consistent with earlier higher pressure selected ion flow tube (S1 'T)

observations[3,4], in which the association reaction was noted to proceed with a two-body reaction rate coefficient of 2 x 1 0^{-9} $cm^3 s^{-1}$, at a helium pressure of 0.5 Torr. When M = HCN, the reaction rate coefficient increased to k_3 = 1.1 x 10^{-23} $cm^6 s^{-1}$ [5]. The results for collisional stabilization of $(CH_3NCH^+)^*$ by He were also examined in a variable temperature SIFT-Drift study by Smith and Adams[6] with the similar results to the earlier SIFT study. Elevating the temperature to 580K resulted in the three-body rate being reduced to $k_3 = 3 \times 10^{-26}$ $cm^6 s^{-1}$, when He was the third-body. A similar decrease in the three-body rate was accomplished by increasing the kinetic energy of the methyl ion[6].

A very different result was presented by Kemper, Bass, and Bowers[7] in 1985. They followed the three-body stabilization reaction from 1 x 1 ()-4 Torr to 1 x 10^{-5} Torr and found only an upper limit of $k_2 = 5 \times 10^{-12}$ $cm^3 s^{-1}$ for the radiative association channel. The reaction rate coefficient they measured for the three-body reaction with He was k_3 = 2.2 x 10^{-25} $cm^6 s^{-1}$. This set of experiments was carried out in a tandem ICR-Dempster-ICR spectrometer where the ion source was separated from the reaction region and only the reaction region contained HCN. The authors concluded that[7]

> "The CH_3^+ + HCN → $[CH_3^+ \cdot \cdot HCN]$ association reaction has been reexamined by using both tandem ICR and drift ICR spectrometers. It appears that the fast radiative stabilization channel reported previously was due to interfering bimolecular reactions and that radiative stabilization dots not occur to a significant extent in this system; i.e. any low-pressure bimolecular rate coefficient must be less than ~5 x 10^{-12} cm^3 s^{-1}."

All the three-body reaction studies at low pressures (<1 0-3 '1'err) used both the parent ion abundance, CH_3^+, and the product ion abundance, $C_2H_4N^+$, to determine the reaction rate coefficient. This differs from the radiative association rate constant measurements measured in the trapped-mode ICR experiments, where only the CH_3^+ ion was followed. In point of fact at no time has the presence of a product

ion for the "radiative association" reaction been accounted for in the ICR trapped mode experiments.

A MIKES-CID study[8] was able to show that at high pressure (10-4 "1'err) the low energy collisionally stabilized products had the structure of CH_3CNH^+. At lower pressures ($<10^{-5}$ Torr) the adduct ha I a structure like that of CH_3NCH^+.

Gilbert and McEwan[9] and Smith *et al.*[10] using RRKM methods, modeled the CH_3^+/HCN system. The model was found to be very sensitive to the structure of the collision complex and the transit on state back t o reactants. They concluded that the CH_3NCH^+ is the structure of the association product that best fits the kinetic data of both the ICR and SIFT, even though the CH_3CNH^+ structure has the lower heat of formation.

Results of four different experiments will be presented and discussed. Two will bc the results of the low-pressure trapped-mode ICR and FT-ICR experiments between 10^{-7} and 10^{-6} Torr. The other two results will be higher pressure results from drift-mode ICR and tandem ICR-Dempster-ICR experiments between 10^{-5} and 10-3 Torr. An interpretation will be presented and applied to the observations from the four different experiments.

The ncw experiment is the FT-ICR. A reexamination of the tandem ICR-Dempster-ICR experiment will also be presented.

EXPERIMENTAL.

'l'he trapped-mode ICR and drift-mode ICR experiments were n o t performed as part of this work. Descriptions of these experiments can b e found in the references cited.

FT-ICR

The FT-ICR experiments were performed using an OMEGA 50 Ion Spec[11] Fourier Transform Mass Spectrometer. Briefly, the instrument utilized computer controlled digital FT-ICR technology. Special features of this instrumentation included: sequential multiple double resonance ejection, pulsed gas inlet system, and a 10" Walker Scientific electromagnet. The magnetic field was typically 1.1 Telsa. The cell was a

single 5.() cm cube. Electron impact ionization was used to initiate ionization. The cell was pumped by a Balzer 330 1 s^{-1} turbo molecular pump.

Tandem ICR-Dempster-ICR

This instrument was built at UCSB and has been described previously[12]. "It has been relocated to J] 'I. (see acknowledgments.)

The design is an adaptation of that used by Smith and Futrell[13]. Instead of the standard Dempster source an ICR ccl] was used as the ion Source. ions generated in this cell are accelerated to typically 3000 volts ant] bent through 180 degrees. A second ICR cell is located 4.74 cm from the first, the 15 Dalton ions are guided into this second ICR by adjusting the magnetic field. The ions are, decelerated and introduced into the second ICR through a (),5 mm thick Wein filter which is 3.8 mm long. "l'his design only allows ions with less than ().3 eV of translational energy t o enter the detection ccl]. A Wronka bridge detection circuit[14] was used t o measure the ion abundances within the detection cell.

RESULTS AND DISCUSS1ON

Trapped-mode ICR

Typical results of experiments reported earlier from our laboratory[1,2] arc shown in Figure 1. The experiment consisted of recording CH_3^+ ion densities at different trapping times for known pressures of HCN in the ICR cell. The reaction rate coefficients for t h e reaction of CH_3^+ with HCN were found from the slope of the semi-log pl ot of CH_3^+ abundance, against the trapping time. Analysis of many such decays resulted in the reaction rate coefficient of 2 x 10-10 ±10% $cm^3 s^{-1}$. A typical mass spectrum of the. ions in the ICR cell is shown in Figure 2, The ions present arc at masses 15, 16, 17, 2.6, 2.7, 28, 29, 38, 39, 40, 41, 42, and 43 Daltons. These correspond to the ions: CH_3^+, CH_4^+, CH_5^+, $C_2H_3^+$, CN^+, HCN^+, $HCNH^+$, $C_2H_2^+$, $C_2H_3^+$, $C_2H_4^+$, $C_2H_5^+$, CH_2CN^+, $C_3H_4^+$, $C_3H_5^+$, CH_3CNH^+, and $C_3H_7^+$. The pertinent react ions[15] in the ICR cell arc

then:

$$CH_2^+ + HCN \rightarrow CH_2CN^+ + H \quad (3)$$

$$CH_2^+ + CH_4 \rightarrow C_2H_2^+ + 2H_2$$
$$\rightarrow C_2H_3^+ + H_2 + H$$
$$\rightarrow C_2H_4^+ + H_2$$
$$\rightarrow C_2H_5^+ + H \quad (4)$$

$$CH_3^+ + CH_4 \rightarrow C_2H_5^+ + H_2 \quad (5)$$

$$CH_4^+ + CH_4 \rightarrow CH_5^+ + CH_3 \quad (6)$$

$$CH_4^+ + HCN \rightarrow HCNH^+ + CH_3$$
$$\rightarrow CH_3CNH^+ + H \quad (7)$$

$$CH_5^+ + HCN \rightarrow HCNH^+ + CH_4 \quad (8)$$

$$C_2H_2^+ + CH_4 \rightarrow C_3H_4^+ + H_2$$
$$\rightarrow C_3H_5^+ + H \quad (9)$$

$$C_2H_2^+ + HCN \rightarrow HCNH^+ + C_2H$$
$$\rightarrow CHCCNH^+ + H \quad (10)$$

$$C_2H_3^+ + CH_4 \rightarrow C_3H_5^+ + H_2 \quad (11)$$

$$C_2H_3^+ + HCN \rightarrow HCNH^+ + C_2H_2 \quad (12)$$

$$C_2H_5^+ + CH_4 \rightarrow C_3H_7^+ + H_2 \quad (13)$$

$$C_2H_5^+ + HCN \rightarrow HCNH^+ + C_2H_4 \quad (14)$$

$$CN^+ + CH_4 \rightarrow CH_3^+ + HCN$$
$$\rightarrow CH_4^+ + CN$$
$$\rightarrow HCN^+ + CH_3$$
$$\rightarrow HCNH^+ + CH_2$$
$$\rightarrow CH_2CN^+ + H_2 \quad (15)$$

$$CN^+ + HCN \rightarrow HCN^+ + CN$$
$$\rightarrow C_2N_2^+ + H \quad (16)$$

$$HCN^+ + CH_4 \rightarrow HCNH^+ + CH_3$$
$$\rightarrow C_2H_3^+ + NH_2 \quad (17)$$

$$HCN^+ + HCN \rightarrow HCNH^+ + CN \quad (18)$$

Of the ions produced in the ICR cell by electron impact and the reaction sequence (3) through (1 8), the protonated hydrogen cyanide ion, $HCNH^+$ is the most abundant. Using the double resonance technique all of Reactions (3) through (18) could be verified, but the product ion of Reaction (1) could not be confirmed. On several occasions double

resonance experiments indicated a small fraction of the $HCNH^+$ ion was derived from CH_3^+, but this was not reproducible. A problem inherent in establishing a double resonance link between CH_3^+ and $HCNH^+$ is that the 28 Daltons signal is very large due to primary ionization of HCN and subsequent proton transfer to HCN.

FT-ICR

These results are new. We were able to observe the reaction of CH_3^+ with HCN using FT-ICR technology on an IonSpec FT-ICR mass spectrometer[11]. The methyl ion was generated by electron impact on methane in a one cell instrument with HCN present during the whole experiment. A pulsed valve was used to introduce the methane into the spectrometer. The valve was open for 2 milliseconds. After a delay of 80 milliseconds, a 5 millisecond pulse of electrons was used to ionize the gases. in a resultant mass spectrum ions were identified at 15, 16, 17, 27, 28, 29, and 42 Daltons. Minor peaks at 18 and 19 Daltons were also present. The mass spectrum at this stage was identical to the trapped-mode ICR experimental results. All ions were then ejected from the cell by sequential double resonance ejection except the CH_3^+ ion at 15 Daltons. The ejection sequence started fifteen milliseconds after the electron pulse and lasted for about 16 milliseconds. The reaction of CH_3^+ and HCN were then allowed to proceed and the ions in the cell were monitored for the next 210 ms as they reacted. Figure 3 shows the results of one of these experiments. It is noted that the methyl ion concentration decreases exponentially with time, while the protonated HCN species increases. The protonated methyl isocyanide product, representing the collision complex and the radiative association product ion, stays at a steady state level of a few percent. We also found the $HCNH^+$ ion signal decreased when the CH_3^+ ion was ejected using a double resonance rf field as it also did when the 42 Dalton ion was irradiated. This second observation of a decrease in $HCNH^+$ upon double resonance ejection of $(CH_3NCH^+)^*$, indicates some $HCNH^+$ ions are derived from CH_3NCH^+, via the Reaction (19).

$$CH_3NCH^+ + HCN \rightarrow HCNH^+ + CH_3NC \qquad (19)$$

Although Reaction (19) is endothermic by 1.48 kJ/mol. for reactants in their ground states, the formation process for CH_3NCH^+ in Reaction (1) is so exothermic that the CH_3NCH^+ ion should have sufficient excess internal energy to drive the reaction. Several other reactions were considered linking the CH_3^+ ion to the $HCNH^+$ ion, but Reaction (19) was the least endothermic option.

These observations allow us to present the following mechanism to represent the reaction sequence in the system.

$$CH_3^+ + HCN \leftrightarrow (CH_3NCH')'' \quad (20)$$

$$(CH_3NCH^+)^{**} \rightarrow (CH_3NCH^+)^* + h\nu \quad (21)$$

$$(CH_3NCH^+)^{**} + M \rightarrow CH_3CNH^+ + M \quad (22)$$

$$(CH_3NCH^+)^* + HCN \rightarrow HCNH^+ + CH_3NC \quad (22)$$

$$CH_3CNH^+ + HCN \rightarrow \text{no reaction} \quad (23)$$

A model based on Reactions (20) through (23) is plotted in Figure 4, We note that in this model the collision complex $(CH_3NCH^+)^{**}$ can be stabilized by either radiative association or collision stabilization, The collisionally stabilized CH_3CNH^+ is not reactive with HCN, while the radiatively stabilized $(CH_3NCH^+)^*$ is. The results of two further experiments were examined to test the proposed mechanism.

Drift-mode ICR

The drift-mode ICR results we have called on were extracted from literature sources[2,5,7]. The experiments consist of observing the parent ion and product ions as a function of the ccl] pressure. The CH_3^+/HCN system has been examined in this way for the parent neutral, HCN, as well as other third bodies like He, Nc, and Ar. The analysis performed was to measure the peak heights of both the reactant and the products and using the power absorption equations to determine an effective second order reaction rate coefficient. The effective second order reaction rate coefficients were then plotted against the third body pressure, Figure 5

shows these results and reveals that the effective second order reaction rate coefficients increase linearly with pressure in this range and have an apparent zero intercept. This observation appears at first to indicate that the association reaction is third order and has no measurable second order reaction rate coefficient. This was in fact the conclusion of Kemper, Bass and Bowers[7] on viewing their results, The drift-mode operation of the ICR results in the reaction sequence (3) through (18) competing simultaneously with reactions (20) through (23). The mass spectrum shown in Figure 6 demonstrates the multiple ion problem under typical drift-mode conditions,

To confirm their predictions, Kemper, Bass and Bowers[7] used the tandem ICR-Dempster-ICR instrument which avoids complications of multiple many ions and neutrals that occur in the reaction region of a single ccl] instruments.

Tandem ICR-Dempster-ICR

The results we present from this instrument are from one previous study[7] plus some new results using the same instrument as in the earlier study. The literature results from the tandem instrument were entirely consistent with the drift-mode ICR results, in that collisional stabilization of the association complex is found to be very efficient. These earlier results which are characteristic of both the drift-mode ICR and tandem instruments, are shown in Figure 5 and present the variation in effective second order reaction rate coefficient with the third body pressure. There is an important distinction between the drift-mode ICR and the tandem instruments. In the tandem, the ion source is completely separate from the reaction region, Methyl ions are generated in the source ICR cell from either methane of methyl bromide. The Dempster section transfers t h c methyl ions from the source cell into the ICR reaction-detection cell. HCN at a known pressure. is added into the reaction-detection ICR cell and the reactant and product ions are all monitored.

With this configuration it becomes possible to detect very low densities of the product ions that have more than one source of production. The model that we proposed in Reactions (20) through (23) for the association of CH_3^+ and HCN, as well as the results of the

experiments with the FT-ICR instrument, suggest that $HCNH^+$ is the product of the proton transfer reaction between the radiatively stabilized collision complex $(CH_3NCH^+)^*$ and HCN. As we have noted earlier, other sources of $HCNH^+$ in single cell instruments obscure this reaction product. Our new experiments with the tandem did show low concentrations of $HCNH^+$ as predicted by the model. A mass spectrum of the ions seen in the tandem experiment is shown in Figure 7. The abundances of ions at 1 S, 28, and 42 Daltons were recorded at different HCN pressures and their measured abundances are compared with calculations based on the model presented in Reactions (20) through (23) in Figure 8. The points are experimental and the lines are the model calculations. Finally we have shown in Figure 9, the relative amounts of CH_3NCH^+ predicted by the model arising from association from complexes stabilized by radiation compared to those stabilized by collision with a third body.

We have noted that the new tandem experiments confirm the predictions of the model, in that a small steady state concentration of $HCNH^+$ was observed in the 10^{-5} Torr range of HCN. The earlier work on the tandem instrument on this system makes no mention of a product at 28 Daltons[7]. Private communication with the authors on this work revealed no evidence that this peak was observed or even looked for. The very low concentrations of the $HCNH^+$ ion would however have made it very easy to have been overlooked. The observation of a very small but nevertheless significant density of $HCNH^+$ is vital for a complete understanding of the stabilization mechanism of the association complex in the CH_3^+/HCN system.

CONCLUSION

We have amalgamated measurements from four different techniques in order to understand the association mechanism between CH_3^+ and HCN. When used in isolation, the conclusions based on evidence from a single technique can be interpreted quite differently than conclusions based on the results of the four techniques taken together. It is the inclusion and extrapolation of results from isolated experimental methods that have led to conflicting statements about the association mechanism

in the CH_3^+/HCN system. The situation is very similar to the Indian fable[16] in which an elephant is examined by six blind men. Each individual touches a different part of an elephant and each reaches a different conclusion as to the nature of the beast.

The amalgamation in this work of the results from all four techniques shows that the simplest mechanism that can explain all the observations is the one given in Reactions (20) through (23). in brief CH_3^+ does react with HCN by a radiative association channel, with a reaction rate coefficient of $k=2x10^{-10} cm^3 s^{-1}$. The association complex also undergoes very efficient collisional stabilization. At the lower pressure ICR experiments (e.g. '1'rapping-mode), reaction times are 100 times longer than the higher pressure ICR experiments (e.g. Drift-mode). Quite different outcomes of the collision complex can eventuate in the different pressure regimes making it difficult to extrapolate the results from one pressure regime to the other, The drift-mode and the tandem results which gave effective zero intercepts on their k_2 versus pressure plots (Figure 5) cannot be interpreted as evidence that radiative association is unimportant in the CH_3^+/HCN system. Rather, it simply reflects the fact that the time between collisions is shorter than the collision complex lifetimes to radiative stabilization,

Finally, we note that the differences in reactivity between radiative stabilization complex $(CH_3NCH^+)^*$ and the collisionally stabilized complex (CH_3CNH^+) are consistent with earlier structural analysis of the products. As noted in the introduction the high pressure MIKE-CID results[8] indicate the collision stabilized product has the CH_3CNH^+ structure. On the other hand Smith et al.[10] found the CH_3CNH^+ structure to be inconsistent with the transition state requirements. It seems reasonable to assume therefore, that the initial stabilized structure is CH_3NCH^+ ion by both stabilization channels which is reactive in the initial energy state towards HCN. Collisions with a third body rapidly isomerizes this to the more stable CH3CNH+ ion which is unreactive towards HCN.

ACKNOWLEDGMENT.

The work described in this paper was carried out at the Jet

Propulsion Laboratory, California Institute of Technology, under contract with the National Aeronautics and Space Administration.

We also again give thanks to Michael "1'. Bowers for his very generous gift of the Tandem ICR-Dempster-ICR instrument, without which this work could not have been completed. We also would like to thank Robert McIver and Rick Hunter for their assistance with the FT-ICR measurements.

1, M. J. McEwan, V. G. Anicich, W. T. Huntress, Jr., P. R. Kemperer, and M. T. Bowers, in Proceedings of IAU Symposium No. 87, *Interstellar Molecules*, cd., B. 11. Andrew, (Reidel, Dordrecht) pp. 305-306 (1980).

2. M. J. McEwan, V. G. Anicich, W. "l'. huntress, P. R. Kemper, and M. T. Bowers, *Chem. Phys. Lett.*, 75, 278 (1 980).

3. 11. 1. Schiff and D. K. Bohme, *Ap. J.*, 232, 740 (1979).

4. H. 1. Schiff, G. I. MacKay, G. D. Vlachos, and D, K. Bohme, in Proceedings of IAU Symposium No. 87, *Interstellar Molecules*, cd., B. H. Andrew, (Reidel, Dordrecht) pp. 307-310 (1 980).

5. L. M, Bass, P. R. Kemper, V. G. Anicich, and M. T. Bowers, *J. Am. Chem. Sot.*, **103**, S283 (1981).

6. D. Smith and N. G. Adams, *Swarms of ions and Electrons in Gases*, Ed. by W. Lindinger, "1'. D. Märk, and F. Howorka, (Springer-Verlag, New York, (1 989), pp. 194-2.17.

7. P. R. Kemper. L, M. Bass, and M, T. Bowers, *J. Phys. Chem.*, **89**, 1105 *(1985),*

8. A, J. Illies, Shuying Liu, and M. 'l'. Bowers, *J. Am. Chem. Sot.*, 103, *5674 (1981),*

9. *R,* G. Gilbert and M, J. McEwan, *Aust. J, Chem., 38,* 231 (198 S).

10. S. C. Smith, M. J. McEwan, and R. G. Gilbert, *J. Chem. Phys., 90, 1630 (1989),*

11. IonSpec Corporation, 17951 Skypark Circle, Suite K, Irvine, California 92714.

12. P. R. Kemper and M. T, Bowers, *Int. J. Mass Spectrom. Ion Phys., 52,*

1, (1983).

13. D. L. Smith and J. H. Futrell, *Int. J. Mass Spectrom. Ion Phys., 14, 171, (1974).*

14. J. Wronka and D. P. Ridge, Rev. *Sci. Instrum.*, **43**, 49 (1982).

15. See V. G. Anicich, *J. Phys. and Chem. Ref. Data, 22, 1469 (1 993).*

16. "The Blind Men and the Elephant," retold by Ellain Quigley (Scribners, New York, 1959),

Figure Captions

Figure 1. Semi-log plot of the methyl ion decay with time. HCN present at 6.0 x 10^{-7} Torr.

Figure 2. Mass spectrum of a methane-hydrogen cyanide mixture as seen in the ICR trapped-mode. Reaction time 75 Ins, HCN pressure 6.0 x 10^{-7} Torr and CH_4 pressure 6.0 x 10^{-7} Torr.

Figure 3. The reaction of the methyl ion with hydrogen cyanide. Using the IonSpec I'-I'-lCR.

Figure 4. Model ion abundance for the conditions of the FT-ICR. The index a refers to products of the collision stabilized channel and the index b refers to products of the radiative association channel.

Figure 5. Plot of the observed 2nd order reaction rate coefficient vs. Bath gas pressure for the reaction of the methyl ion with hydrogen cyanide. Taken from reference 7.

Figure 6. Mass spectrum of a methane-hydrogen cyanide mixture as seen in the ICR drift-mode. Reaction time -1 ms, HCN pressure 4,0 x 10-5 Torr and CH_4 pressure 2.0 x 10^{-5} Torr.

Figure 7. Mass spectrum of a typical ion concentration in the Tandem ICR-Dempster-ICR. Reaction time ~1ms and HCN pressure ~2 x 10-4 Torr.

Figure 8. Data from the Tandem ICR-Dempster-ICR for the methyl ion reaction with hydrogen cyanide, Data points are notes. Lines are from model calculations.

Figure 9. Showing the fraction of the associat on product formed" from collisional stabilization.

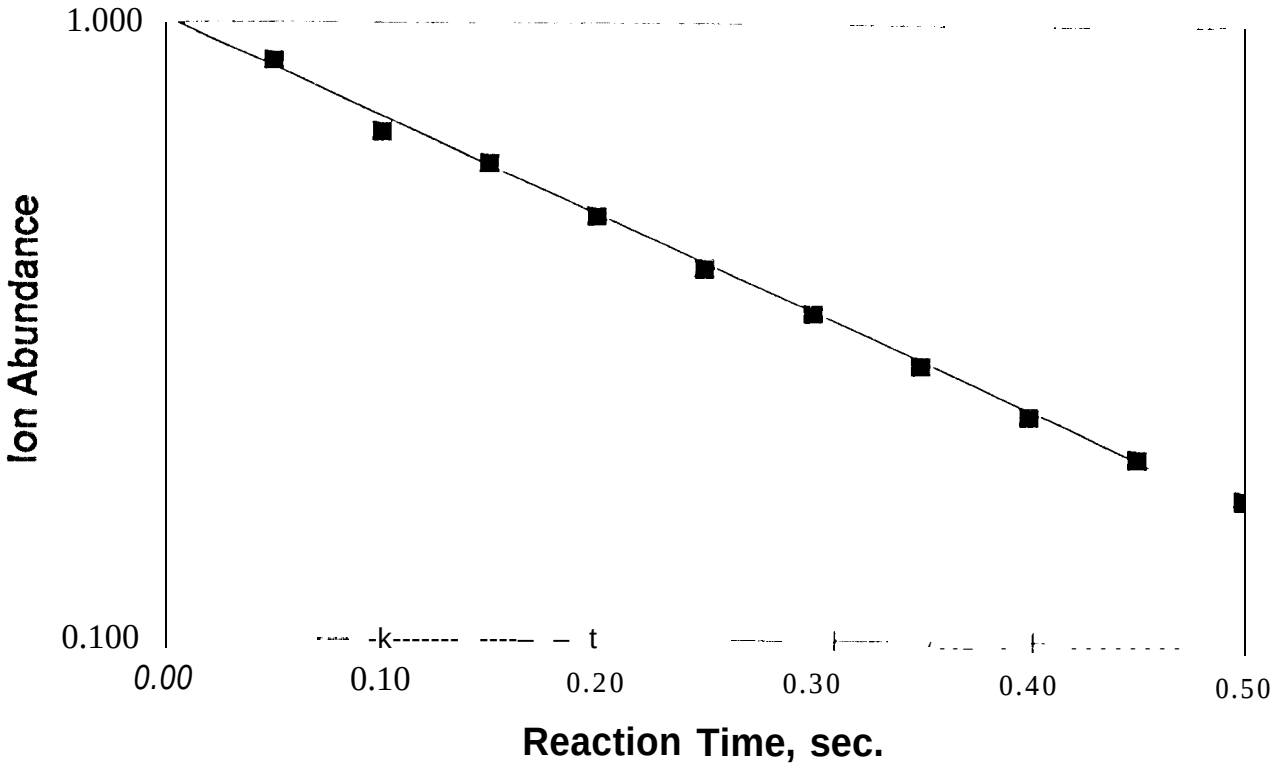

Figure 1. Semi-log plot of the methyl ion decay with time. HCN present at 6.0 xl 0^{-7} Torr.

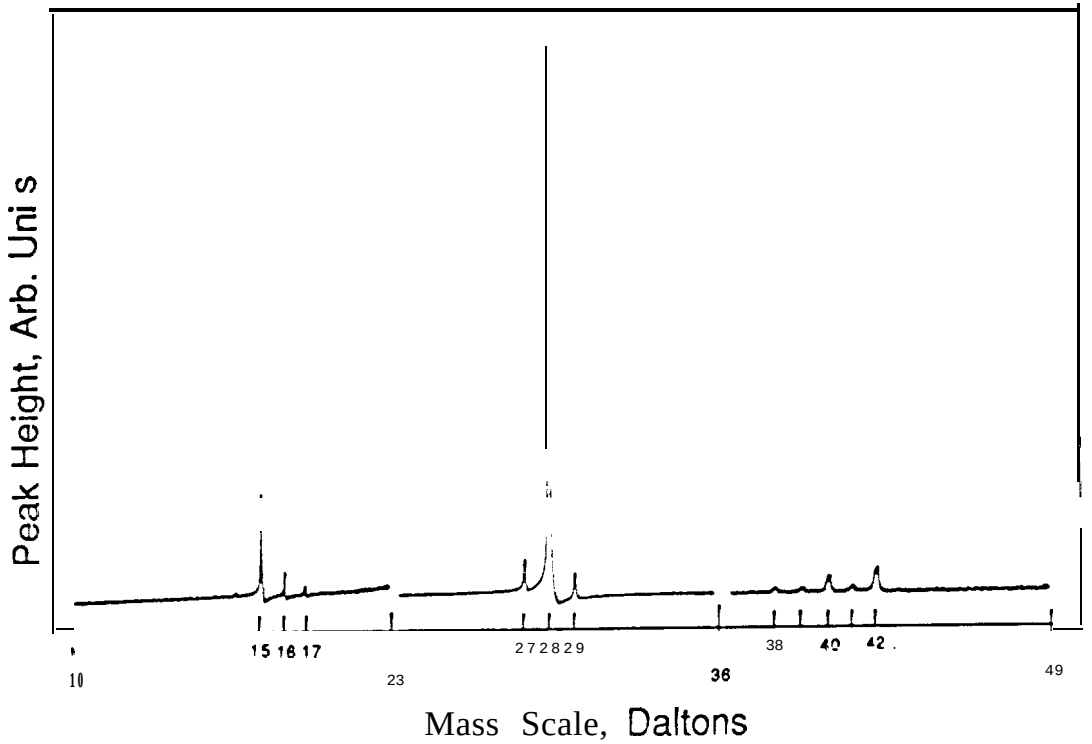

Figure 2. Mass spectrum of a methane-hydrogen cyanide mixture as seen in the ICR trapped-mode.

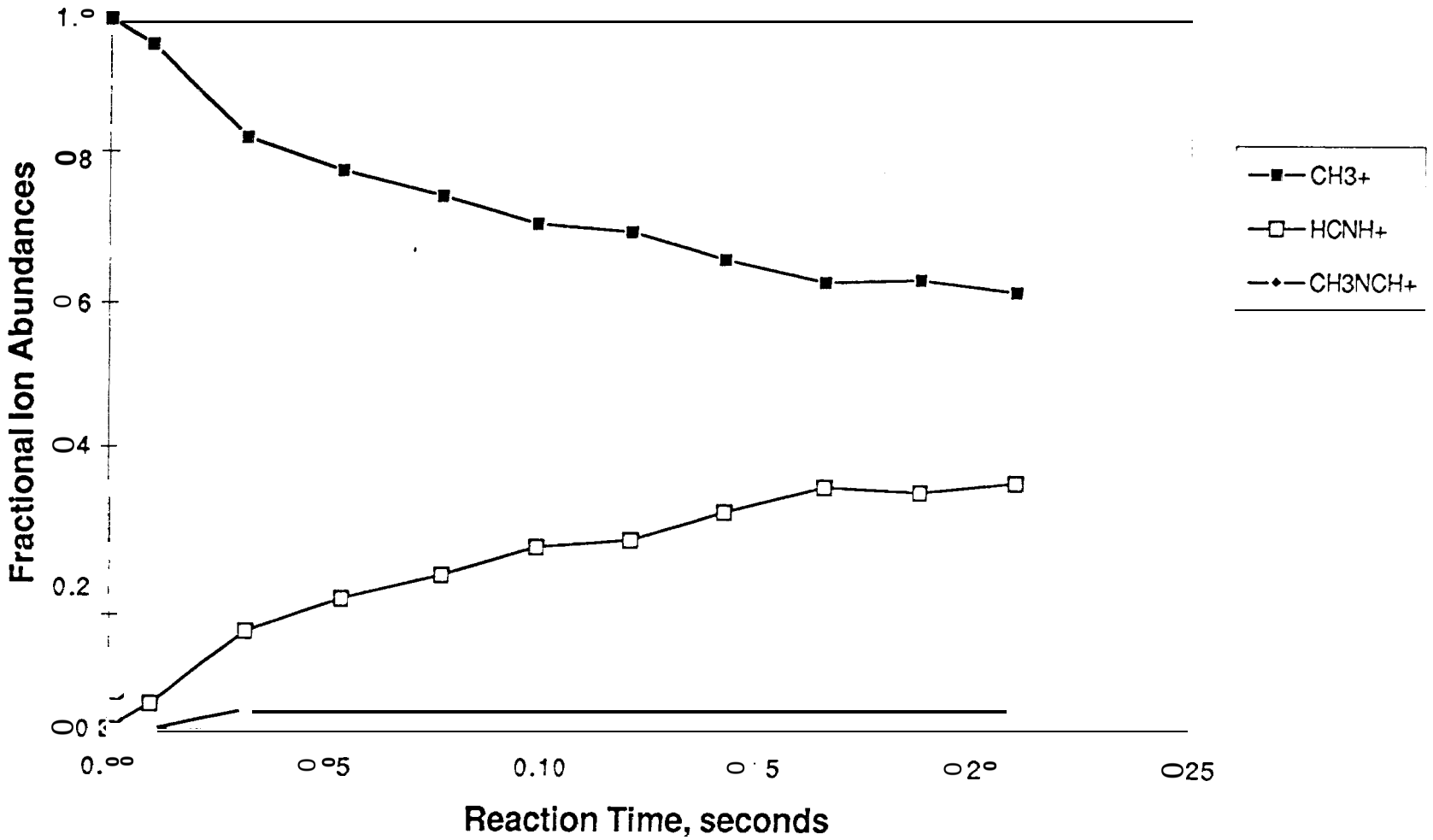

Figure 3. The reaction of the methyl ion with hydrogen cyanide. Using the IonSpec FT-ICR.

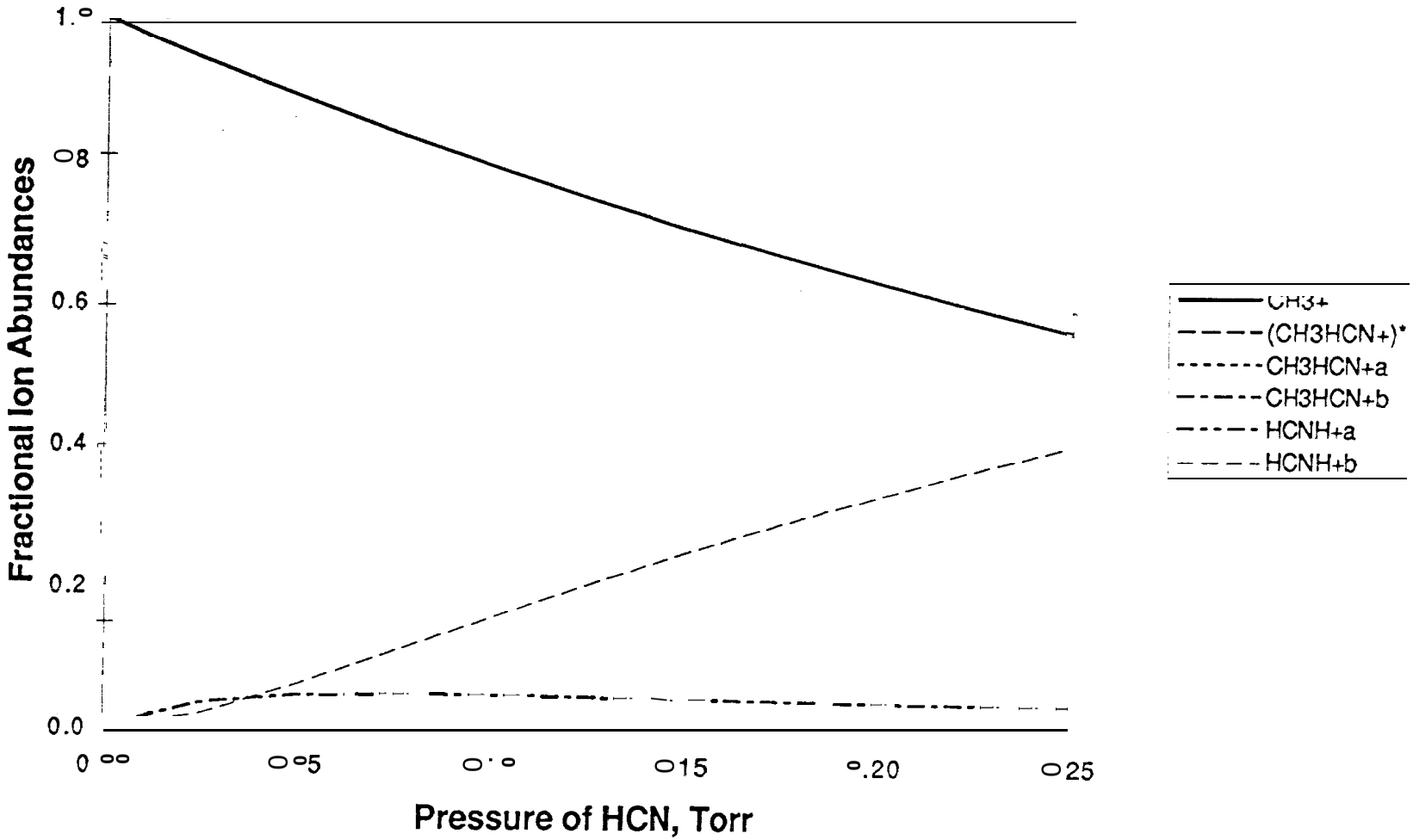

Figure 4. Model ion abundance or the conditions on the FT-ICR. The index a refers to products of the collision stabilized channel and the index b refers to products of the radiative association channel.

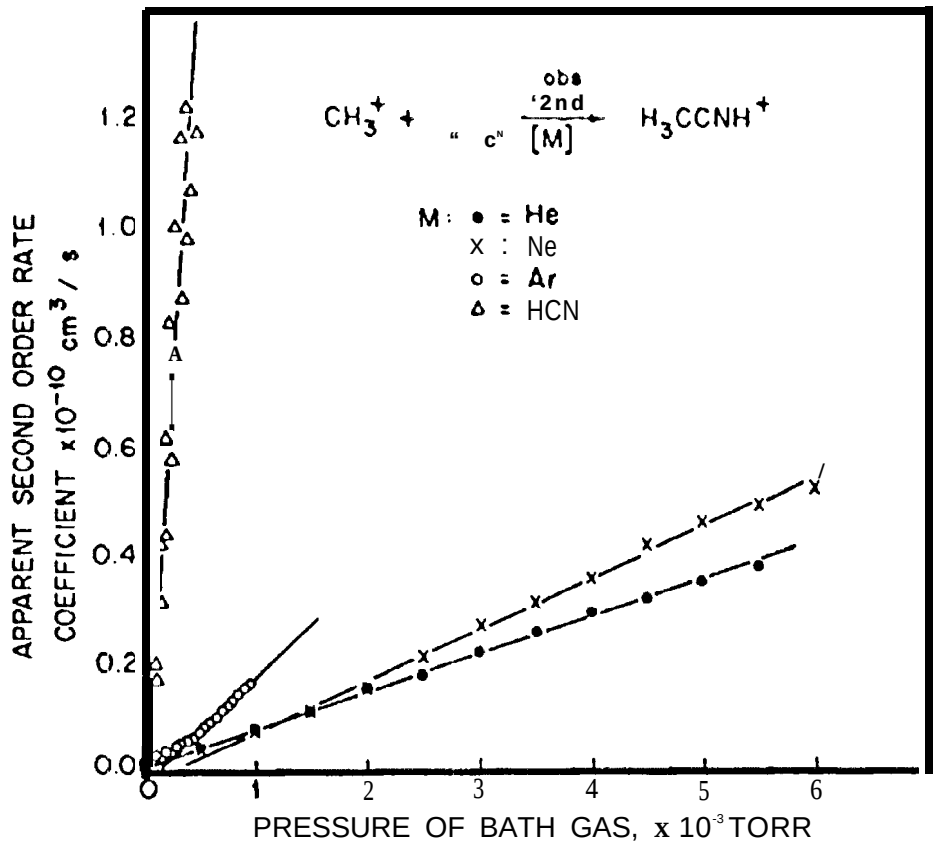

Figure 5. Plot of observed 2nd order reaction rate coefficient vs. bath gas pressure for the reaction of the methyl ion with hydrogen cyanide. Taken from reference 7.

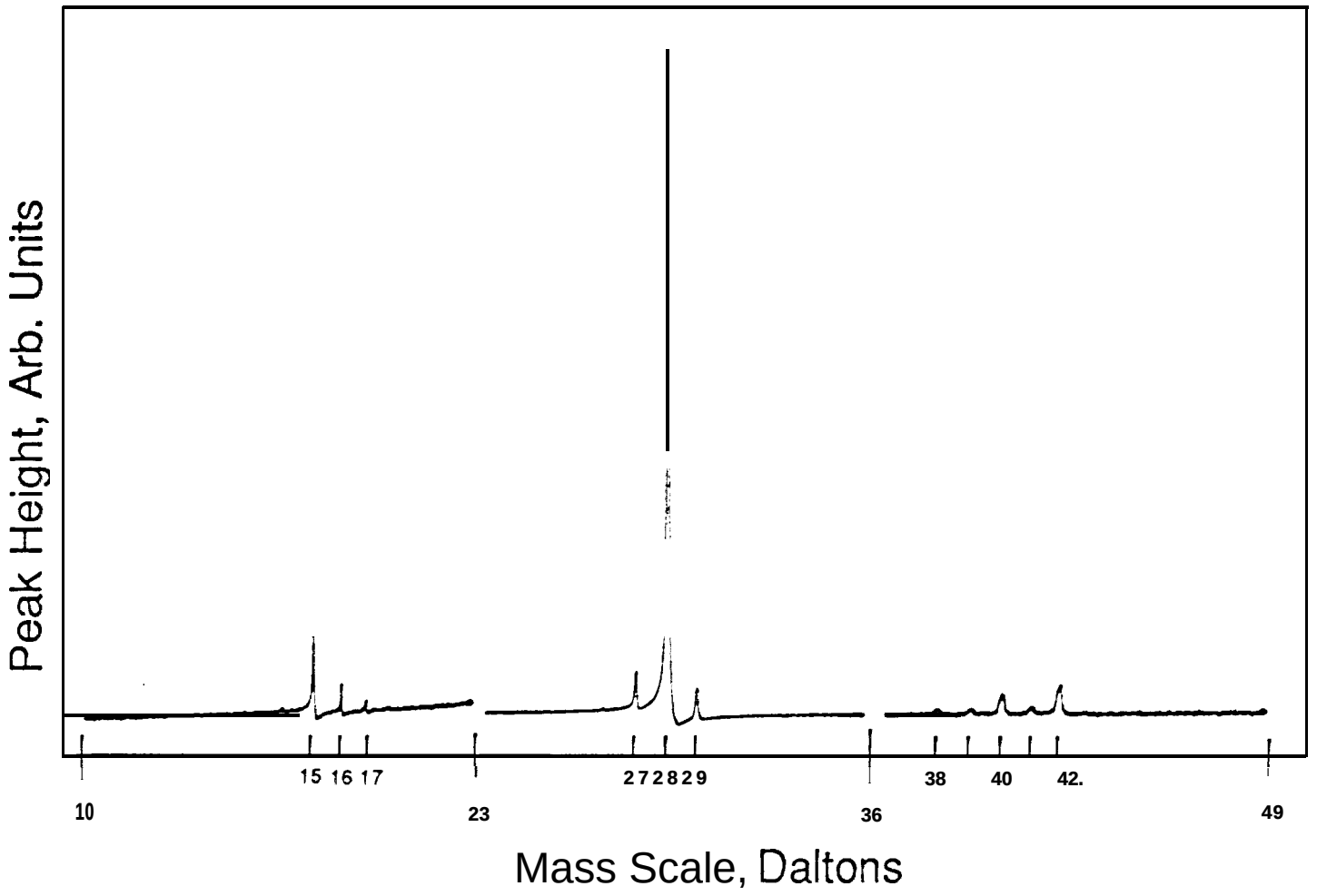

Figure 6. Mass spectrum of a methane-hydrogen cyanide mixture as seen in the ICR drift-mode.

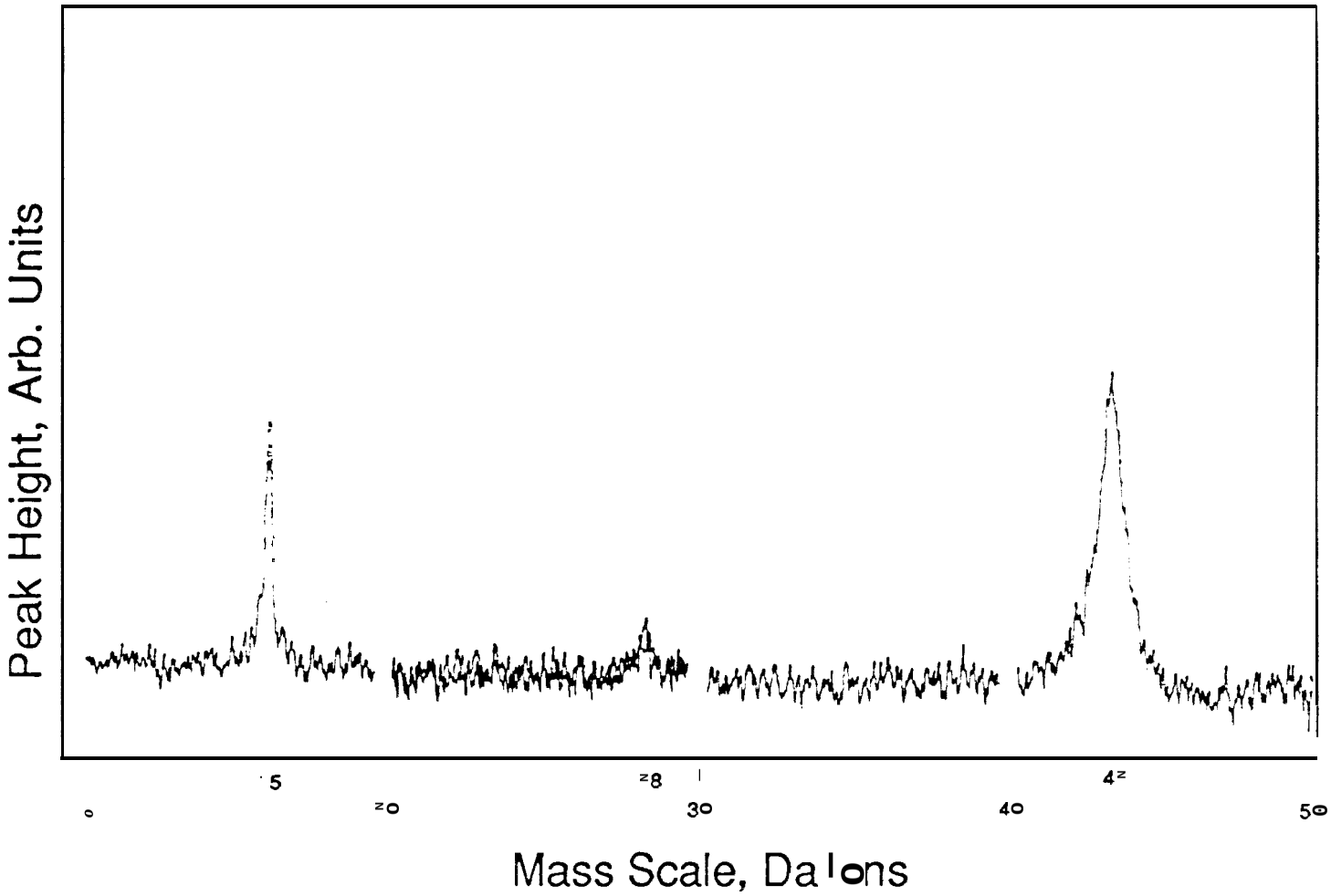

Figure 7. Mass spectrum of a typical ion concentration in the Tandem ICR-Dempster-ICR.

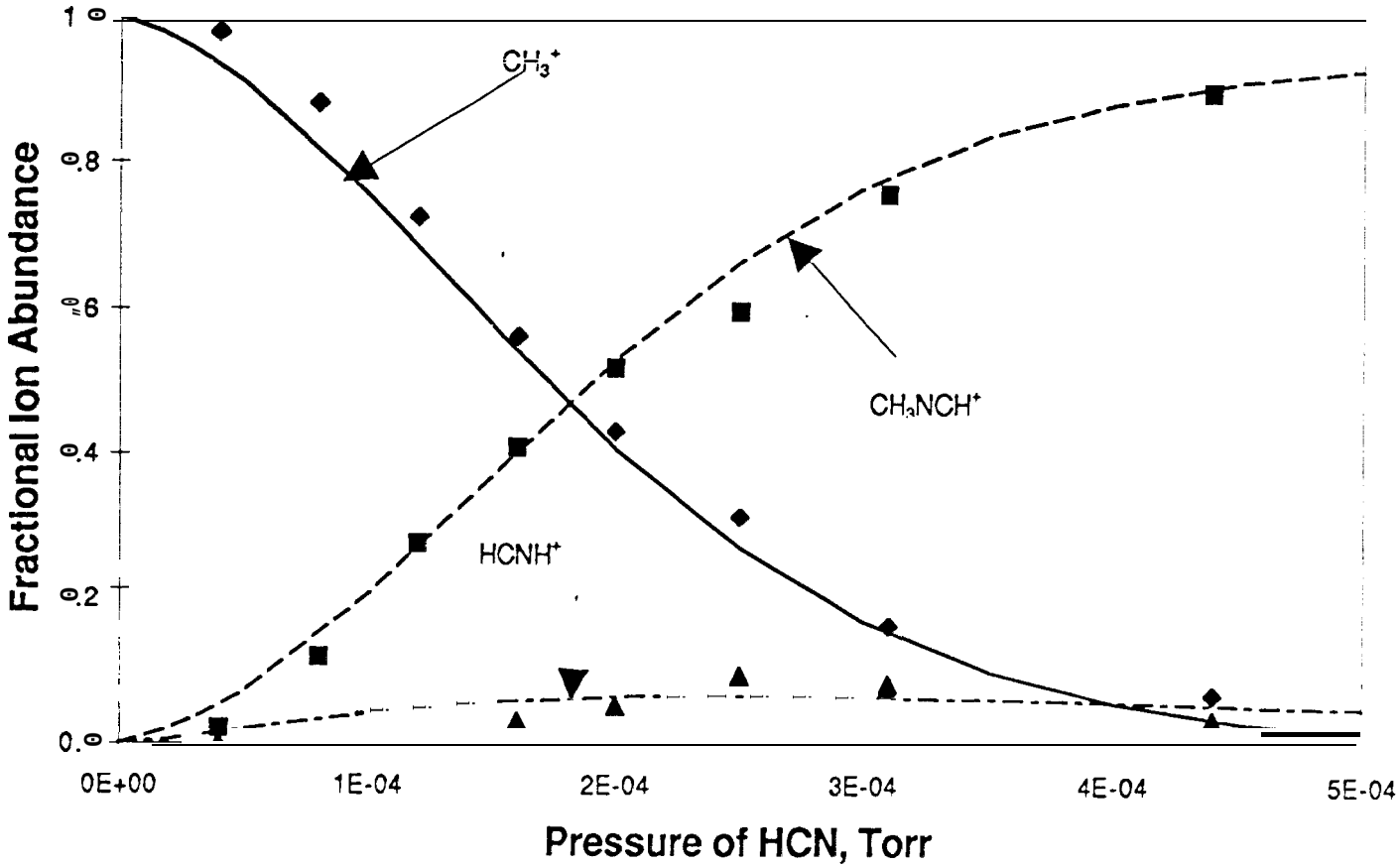

Figure 8. Data from the tandem ICR-Dempster-ICR for the methyl ion reaction with HCN. Data points are noted. The lines are modeled.

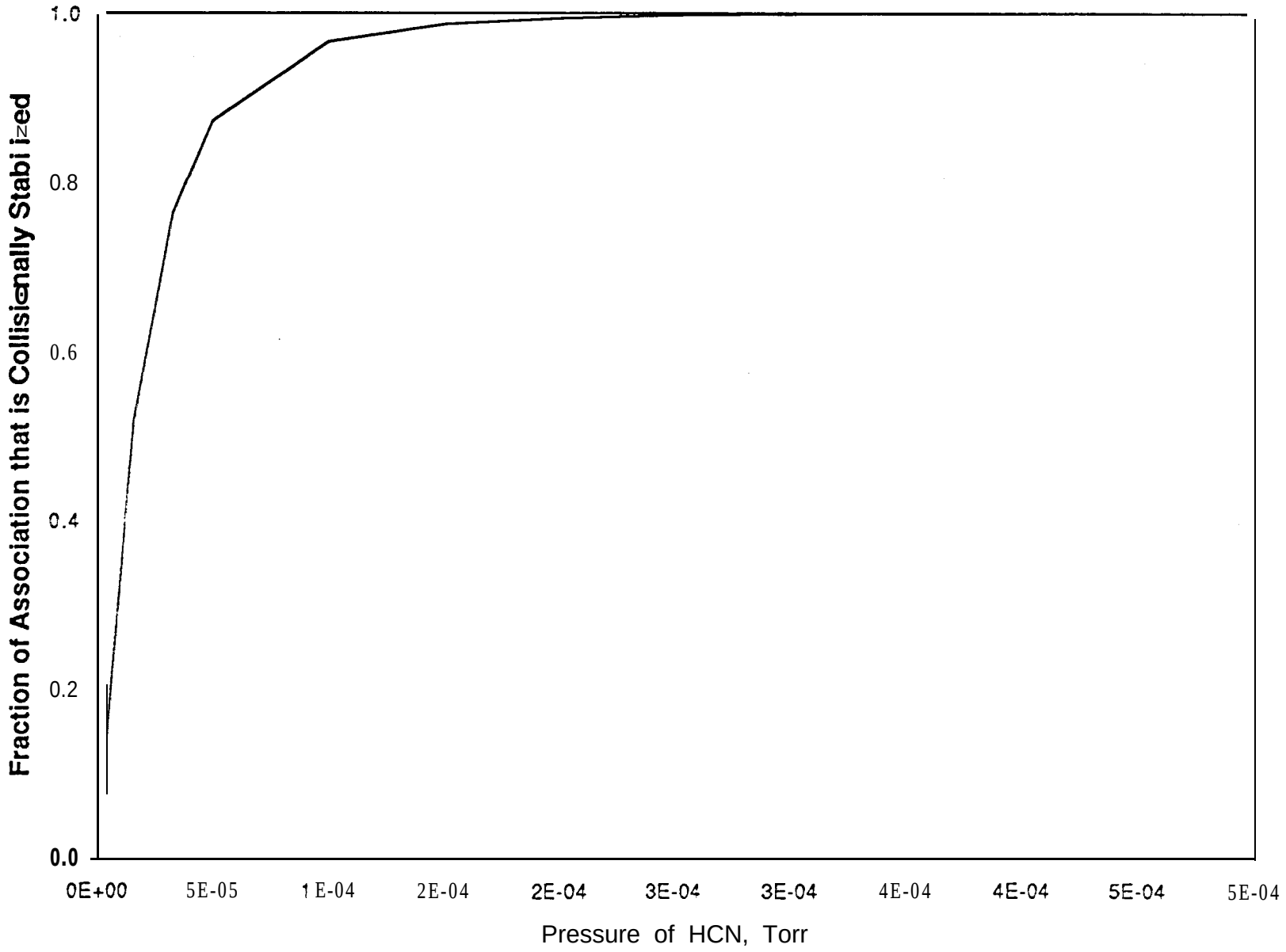

Figure 9. Showing the fraction o' the association product formed from collisional stabilizations